Saudi Journal of Biological Sciences (2017) 24, 787–796

King Saud University

Saudi Journal of Biological Sciences

www.ksu.edu.sa
www.sciencedirect.com

ORIGINAL ARTICLE

Preliminary fabrication and characterization of electron beam melted Ti–6Al–4V customized dental implant

Ravikumar Ramakrishnaiah [a,*], Abdulaziz Abdullah Al kheraif [a], Ashfaq Mohammad [b], Darshan Devang Divakar [a], Sunil Babu Kotha [c], Sree Lalita Celur [d], Mohamed I. Hashem [a], Pekka K. Vallittu [e], Ihtesham Ur Rehman [f]

[a] *Dental Biomaterials Research Chair, Dental Health Department, College of Applied Medical Sciences, King Saud University, Riyadh 11433, Saudi Arabia*
[b] *FARCAMT, Advanced Manufacturing Institute, College of Engineering, King Saud University, Riyadh 11421, Saudi Arabia*
[c] *Department of Pediatric Dentistry, Riyadh Colleges of Dentistry and Pharmacy, Riyadh 11681, Saudi Arabia*
[d] *Department of Oral and Maxillofacial Surgery, College of Dentistry, Princess Noura bint Abdulrahman University, Riyadh 11671, Saudi Arabia*
[e] *Department of Biomaterials Science and Turku Clinical Biomaterials Centre, Professor and Chair of Biomaterials Science, Director of Turku Clinical Biomaterials Centre – TCBC, Institute of Dentistry, University of Turku and City of Turku Welfare Division, Turku, Finland*
[f] *Department of Material Science and Engineering, The Kroto Research Institute, The University of Sheffield, Sheffield S3 7HQ, United Kingdom*

Received 28 February 2016; revised 10 April 2016; accepted 1 May 2016
Available online 7 May 2016

KEYWORDS

Ti–6Al–4V;
Electron beam melting;
Additive manufacturing technology;
Dental implant

Abstract The current study was aimed to fabricate customized root form dental implant using additive manufacturing technique for the replacement of missing teeth. The root form dental implant was designed using Geomagic™ and Magics™, the designed implant was directly manufactured by layering technique using ARCAM A2™ electron beam melting system by employing medical grade Ti–6Al–4V alloy powder. Furthermore, the fabricated implant was characterized in terms of certain clinically important parameters such as surface microstructure, surface topography, chemical purity and internal porosity. Results confirmed that, fabrication of customized dental

* Corresponding author at: Dental Biomaterials Research Chair, Dental Health Department, College of Applied Medical Sciences, P.O. Box 10219, King Saud University, Riyadh 11433, Saudi Arabia. Tel.: +966 531219850.
E-mail address: rramakrishnaiah@ksu.edu.sa (R. Ramakrishnaiah).
Peer review under responsibility of King Saud University.

Production and hosting by Elsevier

http://dx.doi.org/10.1016/j.sjbs.2016.05.001

implants using additive rapid manufacturing technology offers an attractive method to produce extremely pure form of customized titanium dental implants, the rough and porous surface texture obtained is expected to provide better initial implant stabilization and superior osseointegration.

1. Introduction

The introduction of computer-aided design and computer-aided manufacturing (CAD/CAM) into the dental field in early 1980s has provided rapid development for the fabrication of dental restorations (Bibb et al., 2006). Currently, CAD/CAM technology is applied to various specific areas in dental field such as, fabrication of customized dental and maxillofacial implants, copings for metal ceramic and all ceramic restorations (Wu et al., 2010). Traditionally metallic restorations in dentistry are fabricated using cobalt chromium and nickel chromium alloy by conventional lost wax technique. The lost wax technique involves several time consuming steps, such as, (i) designing and fabrication of wax pattern, (ii) wax elimination by burnout procedure, (iii) casting and (iv) finishing. All these steps are tedious and too laborious (Syam et al., 2012; Anusavice, 2003). Dental technicians in their daily practice come across several failures in lost wax technique which includes, wax distortion, casting defects, and casting failures leading to inaccuracy in fitting of framework (Al-Mesmar et al., 1999). With increased demand for esthetics and effective functioning, many prosthetic appliances cannot meet patient needs. CAD/CAM technology has served as a new promising technology and has transformed conventional lost wax techniques to next generation technique, which is more convenient and accurate (Jevremovic et al., 2011).

Presently there are various techniques in CAD/CAM technology, subtractive milling is the commonly employed technique in dental restoration production, where the restoration is milled out of solid block. Alternatively, additive manufacturing (AM) technique which has shown more promising potential in fabricating customized maxillofacial or orthopedic implants and scaffolds, forms the restoration by adding and melting alloy powder by employing layering technique (Chahine et al., 2005; Jamshidiniaa et al., 2014, 2015). AM technique includes electron beam melting (EBM) and selective laser melting (SLM) or laser beam melting (LBM). The EBM utilizes electron beam, whereas SLM utilizes focused 0.2 kW Yb: YAG laser beam to melt alloy powder (Syam et al., 2012; Chahine et al., 2005) and both techniques utilize powder bed fusion (PBF) technology (Syam et al., 2012; Al-Mesmar et al., 1999; Einstein et al., 1963). In SLM the build temperature is maintained at ~90 °C which is comparatively lower than EBM technique. EBM and SLM have individual merits of their own, one of the main advantages of EBM over SLM is the build chamber is enclosed in high levels of vacuum. The vacuum protects highly oxidizing materials such as Ti–6Al–4V. This is unlike SLM, wherein the molten pool is mainly protected by blowing an inert gas that may not be as effective. Moreover, the vacuum helps EBM to be a hot powder-bed process, which means the whole build chamber is maintained at substantially higher temperatures from the ambient conditions. Residual stresses that may arise because of the wide differences in temperatures between the top melting layers and cold bottom can be minimized by hot bed procedure. Another noteworthy advantage of EBM is that, the beam is controlled by electro-magnetic lens, which can be quick acting compared to the mechanical mirror system that controls the laser beam. Hence, the building times can be faster in EBM for the same thickness of each melted layer. Today's AM techniques are able to produce small, complex 3D parts like copings for metal ceramic restorations, metal frame works for partial dentures, dental, maxillofacial and orthopedic implants using different metal powders, such as, cobalt–chromium and medical grade Ti–6Al–4V alloy (Bibb et al., 2006; Al-Mesmar et al., 1999; Jevremovic et al., 2011; Chahine et al., 2005; Einstein et al., 1963).

Pure titanium and titanium alloys are well established standard materials for biomedical applications (Syam et al., 2012). In dentistry, titanium alloys are used to produce dental implants, implant abutments and super structures or copings for overlying prosthesis (Elmagrabi et al., 2008). Since the introduction of titanium implants for dental use, extensive research has been done to optimize its biocompatible and biomechanical characteristics. Ti–6Al–4V is the widely accepted grade 5, alpha–beta, rapidly solidifying titanium alloy for biomedical applications because of its high resistance to corrosion, low heat conductivity, low modulus of elasticity and high tissue bone integration and it is also approved by the American Food and Drug Administration (Syam et al., 2012; De Peppo et al., 2012). This alloy is extremely difficult to cast because of its high melting temperature of 1604–1660 °C and its highly reactive nature at elevated temperatures, casting titanium requires special investment material, careful cooling cycles and special casting equipment. At present, the EBM technique that was introduced by ARCAM AB™ (Gothenburg, Sweden) utilizes Ti–6Al–4V alloy powder to fabricate complex structures under vacuum, preventing the chemical reaction between metal powder and atmosphere (Syam et al., 2012). Furthermore, commercially dental implants are available in limited sizes in terms of its length and width, sometimes these commercially available implants may not match the clinical conditions. Available bone may restrict the surgeon from selecting ideal implant size, hence, there is need for a technology where surgeons can use custom made implants that suite clinical conditions and patient requirements. This will allow fixing implant to the patient, rather than, fixing the patient to implant.

Therefore, this research was aimed to design and fabricate customized root form dental implants using EBM technology. Furthermore, the implants were characterized to study certain clinically important parameters such as surface microstructure, topography, chemical composition, wettability and internal microstructure which are considered crucial for better osseointegration.

2. Materials and methods

2.1. Sample preparation

Root form dental implants of 3 × 10 mm was designed using Geomagic™ (Studio 10, Morrisville, NC, USA), Magics™ (Materialise, Leuven, Belgium, Version 15) and manufactured by EBM technique (A2, Arcam AB™, Krokslatts fabriker 30, Mondal, Sweden). Inert gas atomized, pre-alloyed Ti–6Al–4V powder of particle size 45–100 μm supplied by Arcam AB™, Sweden was used as feedstock material. The powder size is determined by many factors. For instance, a finer powder would give better surface finish because in such a case staircase effect would be minimized. Nevertheless, too fine a powder may destabilize the vacuum inside the build chamber. Hence, a balance has to be struck with respect to the size of the powder. EBM utilizes the electron beam at 60 kV to melt alloy particles under vacuum pressure of 2×10^{-3} mbar in the inert helium environment. The vacuum environment will protect the molten metal from oxidation. In addition to this, the helium environment plays other roles such as stabilizing the electron beam and preventing 'smoke'. 'Smoke' is a phenomenon that can occur during the build process and occurs when too many electrons pile up on the surface of the powder particles. Thus each particle repels one another creating a powder cloud. Too many 'smokes' can result in build failure. The build temperature used was 750 °C and substrate plate temperature was 600 °C. The beam current was set at 17 mA and scanned at a speed of 1473 mm/s. Every time 0.07 mm thick layer of powder was raked during the process.

In the EBM process, an electron beam is accelerated at about 60 kV potential. This beam strikes a layer of powder that is spread by a raking system. Each layer of the powder is fetched by the rake from one of the two hoppers, one on the left side of the build table and the other on the right. Once a layer is melted by the beam selectively, the build table moves down to accommodate a new powder layer. This layering and melting cycle continues until the whole part is built. When the process is completed, the built part has to be post-processed. The built part is removed from the table and taken to a blasting chamber. Here any loose powder particles surrounding the built part are blown away by a blast of pressurized air stream premixed with some amount of the same alloy powder used for the EBM process.

2.2. Characterization

2.2.1. Surface microstructure

External surface microstructure, porosity and particle size of the fabricated root form implants on the build surface and lateral surface were examined by scanning electron microscope (SEM) (JSM-6360LV, JEOL, Japan) at the resolution of 10, 30 and 50X.

2.2.2. Surface topography

Surface topography was measured using optical non contacting surface profilometer (Bruker Contour GT-K™, Bruker nano GmbH, Berlin, Germany). This system utilizes fully automated platform, which is programmable in X, Y and Z directions. This provides high resolution data of the surface characteristics. The simple "Vision64" software translates these high resolution data into accurate 3D image. The surface topography of the specimen was measured by taking the measurements from 6 randomly selected areas on both build surface and lateral surface. To characterize surface topography, the sample was placed on the platform such that the measurement plane was perpendicular to the optical beam. Non-contact surface profilometer uses a laser light spot having a diameter of 1 μm. The measurement length of 1.261 mm and 0.946 mm in X and Y axis respectively and 500 μm in Z axis was taken with a resolution of 100 points/mm in x and y axis, the scanning frequency was 100 points/min and images were captured at 3× optical zoom.

2.2.3. Surface chemical composition

Surface composition was analyzed by laser induced breakdown spectroscopy (LIBS) using Spectrolaser 7000™ (Laser Analysis Technologies, Australia), equipped with software controlled high power Nd:YAG laser, delay unit, optical spectrometer with CCD camera. The laser beam of wave length 1064 nm at the repetition rate of 10 Hz is used. In order to initiate plasma 100 mJ of laser beam was focused on the sample kept on a rotating stage. The plasma emission was collected after a delay of 2.5 μs with CCD camera connected to a computer controlled spectrometer. The elemental analysis is based on the emission spectra of neutral and ionized excited species. The elemental analysis was carried out as described by Farooq et al. by comparing the relative intensities of the spectral lines (Farooq et al., 2013).

2.2.4. Surface wettability

Surface wettability was determined by contact angle (CA°) measurement at room temperature using Oneattension™ (Biolin Scientific, Espoo, Finland). Wettability of the implant surface was measured on the flat cutting edge surface near the apex of the implant using a sessile drop technique, 2 μL drop of deionized water was dispensed on to the implant surface using a syringe and the CA° measurements were taken. The dynamic CA° was measured by inbuilt software from the time of initial contact till the droplet attained stable value. The images were captured using built in digital camera.

2.2.5. Internal microstructure

The internal structure, surface density, linear density and total internal porosity were measured by micro-computed tomography (micro-CT) using Skyscan 1173™ high energy spiral scan micro CT (Bruker-micro CT™, Kartuizersweg 3B, Kontich, Belgium). The X-ray generator of the micro-CT was operated at an accelerated potential voltage of 95 kV with current of 120 μA using a 0.25 mm brass filter with a resolution of 68.66 mm pixels resolution scan. Projection images were recorded in steps of 0.4° from 0° to 360°. The three-dimensional reconstruction was performed with "Insta Recon™" Software (1800 S, Oak St, Champaign, IL 61820). The beam hardening effect reduction of 30% and 12% Ring artifact correction was used to produce the precise image cross section. The resulted data set of 66.68 micro meter voxels of each cross sections was analyzed with "CT An™" (Bruker-micro CT™, Kartuizersweg 3B, Kontich, Belgium, version 1.13.11.0+) software. The 3D visualization has been done

using "CT Vol™" (Bruker-micro CT™, Kartuizersweg 3B, Kontich, Belgium, version 2.2.3.0).

3. Results

3.1. Surface microstructure

Fig. 1a–d shows the SEM images of the build surface and the lateral surface at different magnifications of the root form dental implant respectively. The lateral surface shows the rough surface with the reproduction of threaded pattern designed using Geomagic and Magics. The build surface is characterized by the presence of more uniformly and completely sintered alloy particles with metallurgical bonding between alloy particles and layers, whereas the lateral surface was characterized by the presence of numerous unmelted and partially melted alloy particles. The size of partially melted alloy particles on the lateral surface ranged from 49 to 104 μm, the build surface was also characterized by the presence of numerous hemispherical micro-porosities measuring from 6.6 to 8.6 μm.

3.2. Surface topography

Fig. 2a and b shows the three dimensional representation of the surface topography of the build surface and the lateral surface. Several areal surface texture parameter values were measured to characterize the surface topography which includes Sa (surface roughness), Sp (the maximum surface peak height), Sv (maximum valley or pit depth), Sz (the sum of largest peak height value and largest pit or valley depth), Sq (root mean square value of the sampling area), Ssk (the measure of skewness or symmetry in roughness), Sku (kurtosis of topography height distribution)/(the spread of height distribution). Mean Sa was considered in this study because this parameter gives the arithmetic mean of the heights of sampling surface. The measured Surface roughness of the build and lateral surface after applying Gaussian filter was 0.682 μm and 3.398 μm respectively.

3.3. Surface chemical composition

The spectral data were recorded from 188 nm to 990 nm in four sets, (i) 188 nm–260 nm, (ii) 260 nm–360 nm, (iii) 360 nm–620 nm and (iv) 620 nm–990 nm. The data were analyzed using "Spectrum Analyzer™ 1.7" (Aaronia AG, Gewerbegebiet Aaronia AG, Strickscheid, Germany) and the graphs were drawn using "Spectrolaser™ 2.1" (Laser Analysis Technologies, Australia) Fig. 3a–d show the spectra of the sample from 180 to 990 nm. The integrated intensities of the strongest line of each detected element were considered as their relative abundance. Varying amounts of Titanium (~88.5 wt%), Aluminum (~6.95 wt%), Vanadium (~3.38 wt%), Carbon (~0.74 wt%), Oxygen (~0.014 wt%), Hydrogen (~0.013 wt%), Iron (~0.25 wt%) and Nitrogen (~0.035 wt%) were found.

3.4. Surface wettability

Fig. 4 shows the gradual decrease in CA° value in relation to time in seconds since the contact of water droplet. The droplet deposited on the surface of titanium implant spreads over the

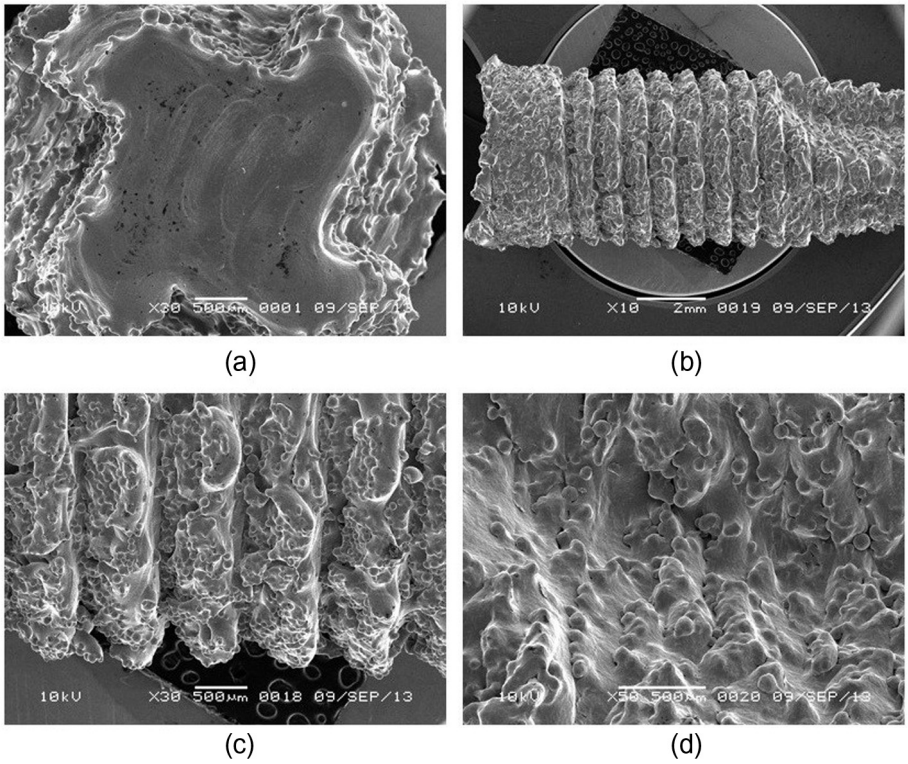

Figure 1 SEM images (a) build surface showing the uniformly melted alloy particles and edge of lateral surface having partially melted alloy particles (b), (c) and (d) lateral surface showing partially melted alloy particles at different magnifications.

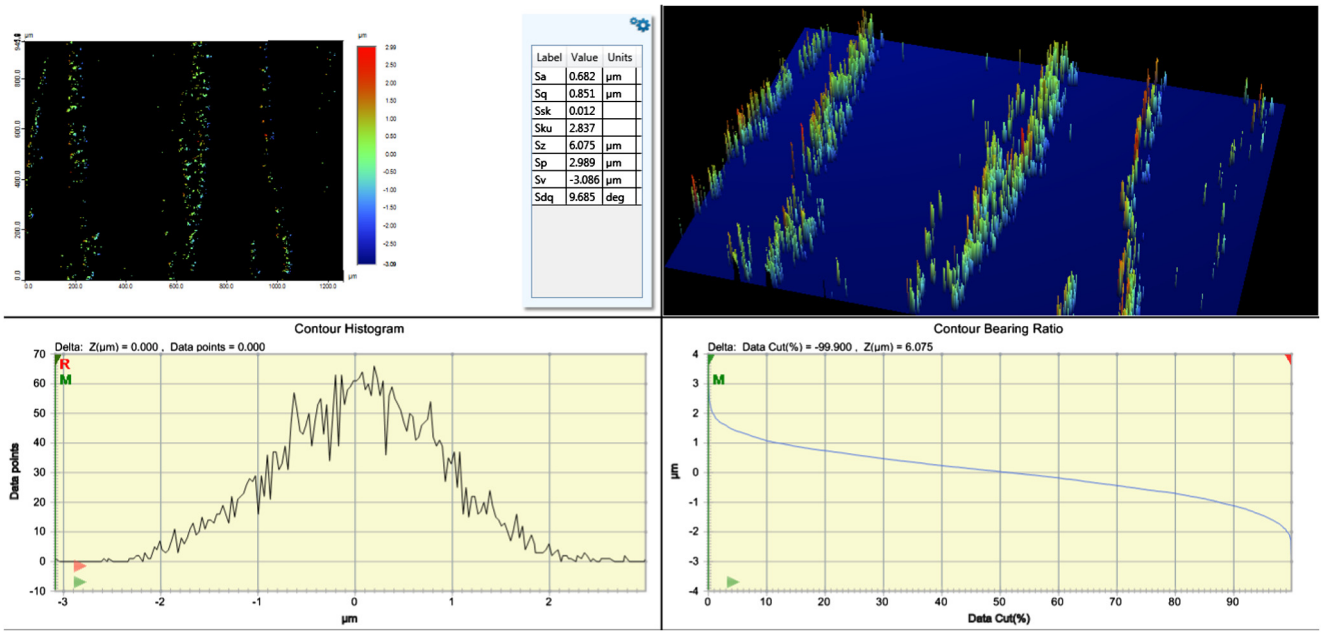

Figure 2a Surface roughness (Sa) of the build surface.

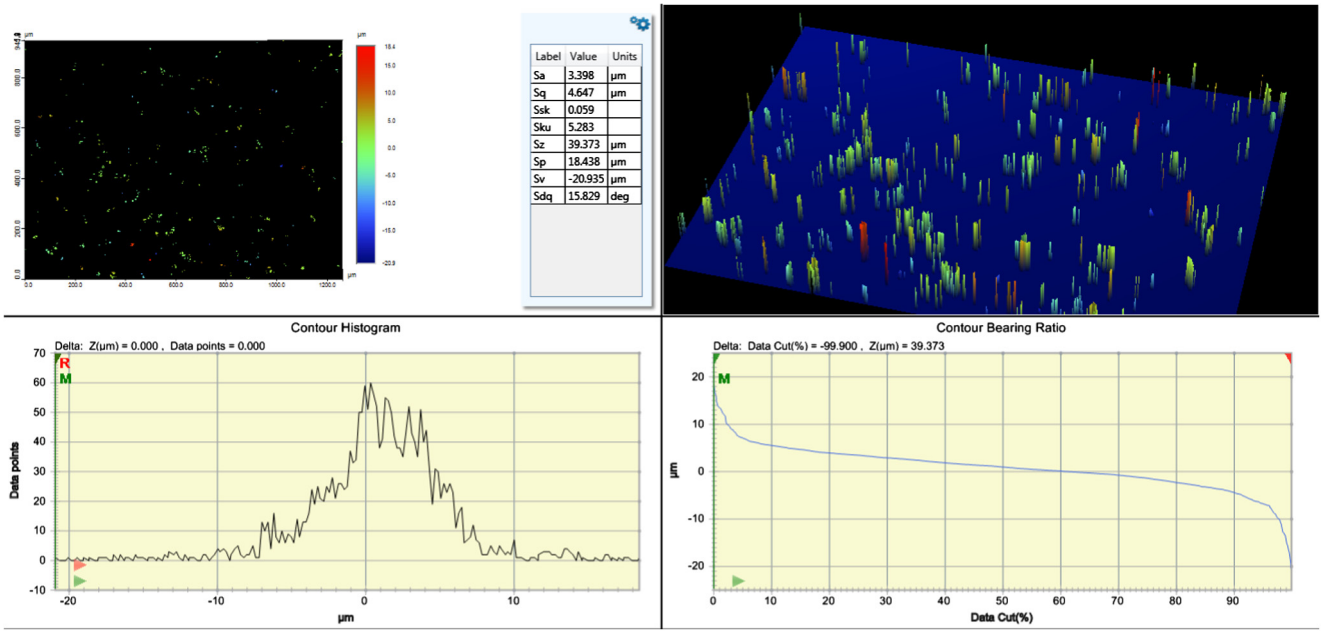

Figure 2b Surface roughness (Sa) of the lateral surface.

surface in a fraction of seconds (Fig. 5) showing CA° value of 6.43, Furthermore in 2 s, droplet reached zero CA° and demonstrated a high degree of surface wettability.

3.5. Internal microstructure

Fig. 6a is the designed implant stl picture and Fig. 6b is the constructed 3D image showing internal porosity from µCT. The fabricated implant when subjected to µCT, scans and takes several longitudinal slices of the implant. The integrated software "Insta Recon™" constructs 3D image from the scans and total internal porosity of the entire constructed 3D image in relation to the total volume was measured using integrated software "CT An™". Structure linear density, surface density and other parameters are tabulated in the table 1. The total internal porosity of the sample was 0.48113%.

4. Discussion

Several attempts have been made to fabricate custom made dental implants and restorations using EBM technology. Chahine et al. designed and produced Ti–6Al–4V extra low

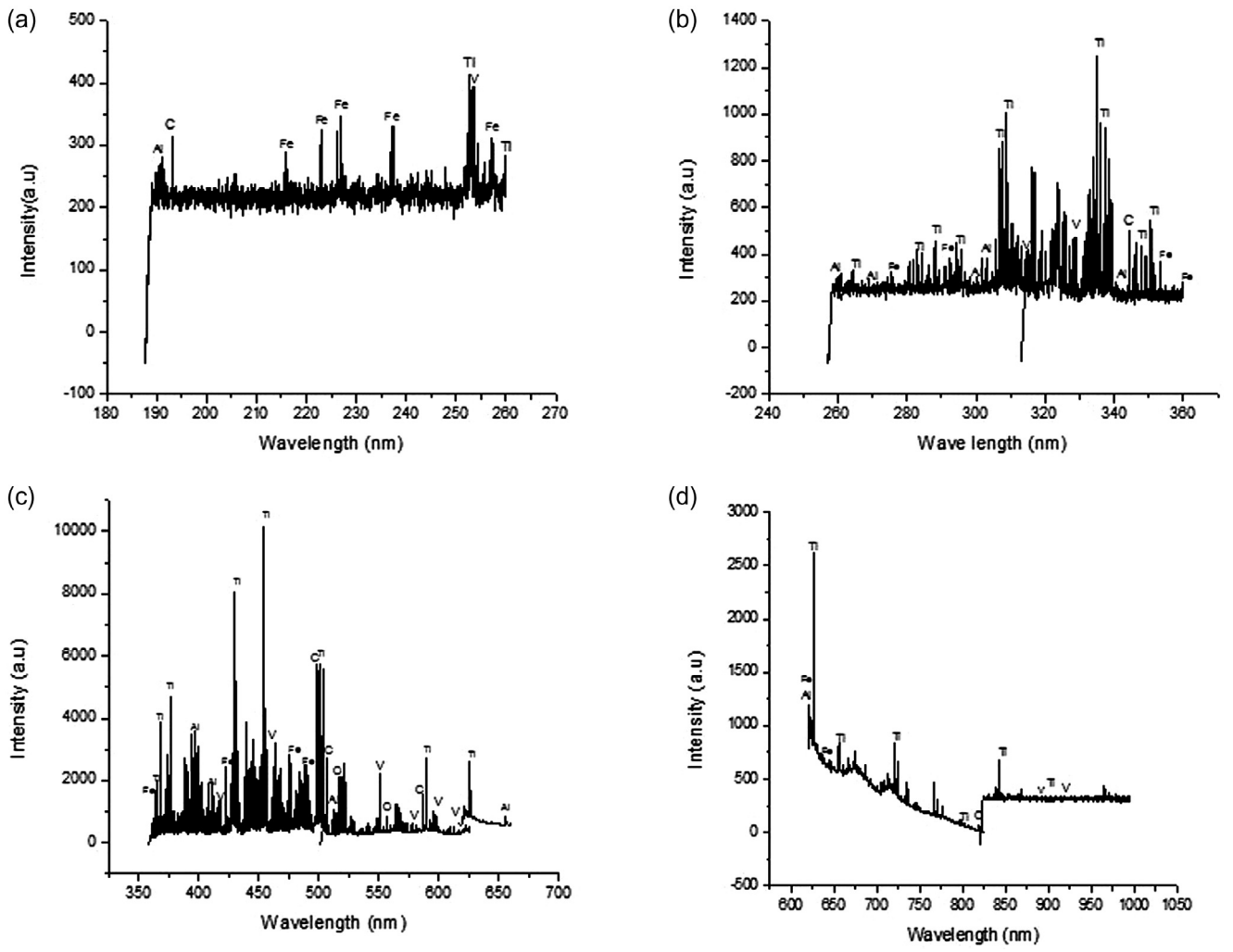

Figure 3 Spectrum of the samples (a) spectrum of the sample from 188 nm to 260 nm (b) spectrum of the sample from 260 nm to 360 nm (c) spectrum of the sample from 360 nm to 660 nm (d) spectrum of the sample from 620 nm to 990 nm.

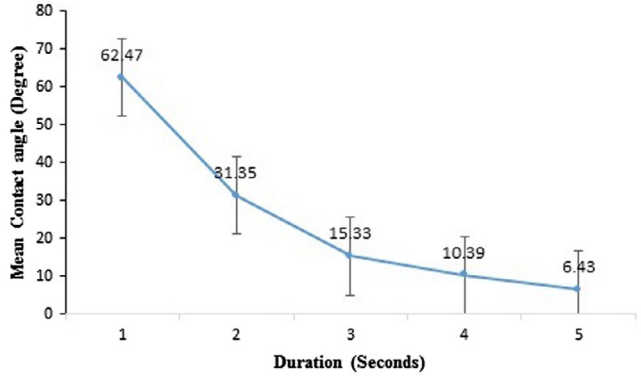

Figure 4 Graph showing gradual decrease in the CA° from the initial contact of water droplet.

interstitial (ELI) customized dental implant and studied some of the mechanical properties and microstructure. They concluded that the mechanical properties were outstanding when compared with the structure produced by casting technique (Chahine et al., 2005). Syam et al. fabricated coping for metal ceramic restoration and studied the shrinkage parameters (Syam et al., 2012). Bibb et al. fabricated a removable partial denture framework using SLM process and concluded that, the accuracy, quality of fit and function were comparable to existing methods (Bibb et al., 2006). Their study showed that, the mechanical properties of the EBM fabricated specimen were lower than the specimens fabricated by LBM technique and wrought specimen. However, the yield strength, tensile strength and percentage elongation were higher than casted specimens. Furthermore, EBM fabricated specimen had higher bulk hardness than LBM, wrought and casted specimens (Koike et al., 2011). Jamshidiniaa et al. fabricated lattice design abutment for dental implant to test fatigue properties. After subjecting to four different cyclic loads, their study results showed that, fabricated lattice design abutment tolerated five million cyclic loading at 100 N. Their study also reported fatigue failure mainly because of partially sintered powder particles and sharp edges on the surface of the structure (Jamshidiniaa et al., 2015). Jamshidiniaa et al. also studied the effect of non-stochastic lattice structure for the dental implant abutment design (Jamshidiniaa et al., 2014). They

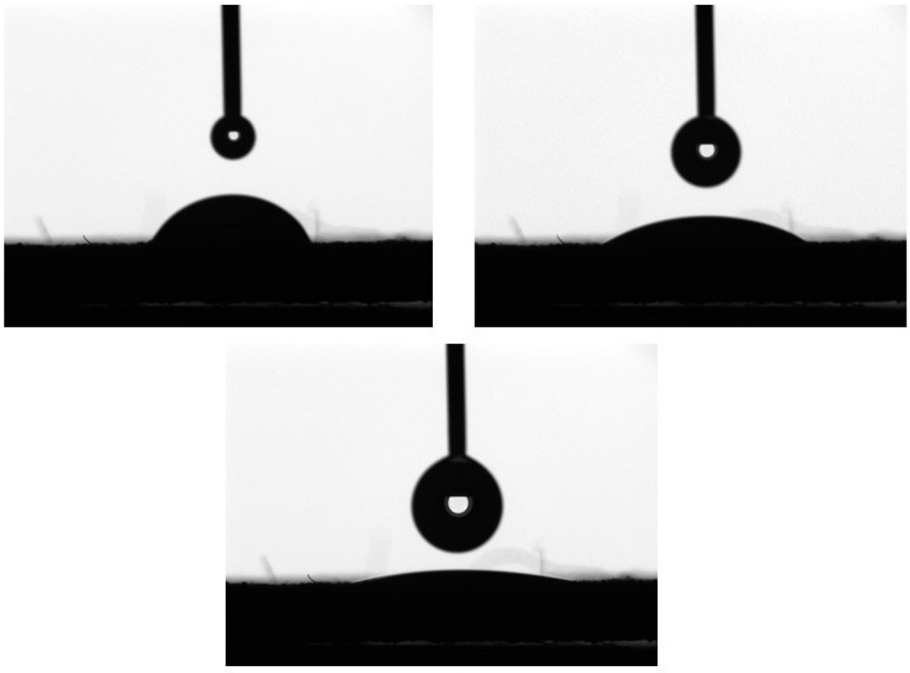

Figure 5 Image showing gradual spread of water droplet.

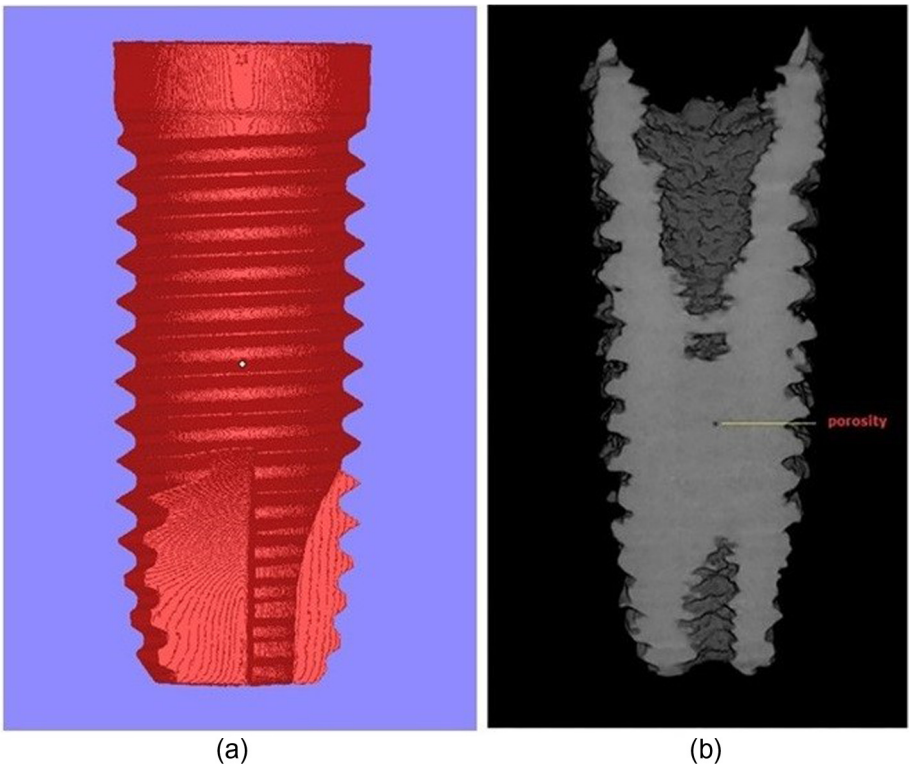

Figure 6 (a) Designed stl. picture (b) Micro CT image of the root form implant taken at the mid-section longitudinal slice, showing dense internal structure and isolated internal porosity.

fabricated a cross, honeycomb and octahedral design with different unit cell size to study the effect of biting force angle on mechanical behavior of lattice abutment. Their study showed increased deformation of the structure under the load with the increase in unit cell size and the numerical analysis showed 30° as a critical biting force angle (Jamshidiniaa et al., 2014). Yang et al. compared the stability and osseointegration of EBM fabricated rough surface with smooth surface titanium

Table 1 Parameters of the sample measured by micro-CT.

Parameters	Values
Object volume	1059.82377 (mm^3)
Structure model index	1.70312
Object surface density	0.62241 (1/mm)
Structure thickness	4.87103 (mm)
Structure linear density	0.20530 (1/mm)
Degree of anisotropy	1.05471
Total porosity	0.48113 (%)

implants. They demonstrated a high degree of osseointegration and torsional resistance to extraction in rough surface EBM fabricated implant (Yang et al., 2014).

The free form EBM built sample fabricated using titanium alloy is widely accepted and biocompatible, having excellent mechanical properties when compared to wrought or casted samples (Murr et al., 2006; Parthasarathy et al., 2010; Heinl et al., 2007). In current research, the specimen typically showed irregular lateral surface and a comparatively smooth build surface as shown by SEM images (Fig. 1a–d), this irregular surface is mainly because of the partial union of alloy particles during the melting process and due to the presence of unmelted alloy particles. This partial union of the alloy particles creates perfect hemispherical porosity on the surface of the structure and represents the external porosity. Some dental restorations require a rough surface, in particular when used as dental implant, this irregular surface which represents external porosity is expected to provide excellent surface for the bone ingrowth, thereby, ensuring strong osseointegration (Heinl et al., 2007,2008; Biemond et al., 2011; Haslauer et al., 2010). With the available software, strut size, shape and porosity size can be adjusted to obtain optimal surface for better osteoblastic adhesion and tissue in growth. The implants surface can be made more porous with mesh or lattice design to have better anchorage with the bone (Murr et al., 2012). The resultant customized surface of the dental implant can also be used to enhance osseointegration in patients with poor bone qualities by incorporating patient specific human embryonic stem cell-derived mesodermal progenitors. Furthermore, commercially dental implants are available in limited sizes in terms of height and diameter. Most of the times, these implants do not suit the clinical conditions, such as bone height, thickness and quality. With the help of EBM technology, the implant can be scanned and specific parameters can be modified to match the clinical conditions (Murr et al. 2009,2010). It has also been reported that the biocompatibility and the biological response of the EBM fabricated structures are relatively high as compared to the implants produced by other techniques (Murr et al., 2010).

Surface chemistry and surface energy of the titanium implant are other important factors that affect osseointegration, as surface impurities impair osseointegration of implants. The surface energy is the result of manufacturing technique; in this research the fabricated structure was analyzed by LIBS, as detection of lighter elements, such as, carbon by standard EDX is difficult (Miguens et al., 2010; Ramakrishnaiah et al., 2012). LIBS detected varying amounts of Titanium, Aluminum, Vanadium, Carbon, Hydrogen, oxygen and Iron. There are two possible ways for loss of chemical species during the EBM process. Titanium which is present in a larger quantity can easily get oxidized at higher temperatures. However, the chances of this happening are slim because, high vacuum levels and the small amount of Helium inert gas protect Titanium. The second and more probable problem that could arise is loss of alloying elements like Aluminum because of their low boiling point as compared to other elements in Ti–6Al–4V. Any changes in Aluminum content would have a significant effect on the microstructure and strength properties of the final part. In our study, the optimized process parameter did not alter the Aluminum content significantly. The Aluminum content was found to be ~6.95 wt% which is well within the range as specified by ASTM standards. Loss of Aluminum occurs if the beam energy is too high, that is well above the melting point of the alloy. Juechter et al. have reported Aluminum content fell as much as 30% when the line energy becomes higher or if the scan speed is too slow. This study emphasizes on the need to employ the right set of process conditions if losses in the chemical elements are to be avoided (Juechter et al., 2014). Furthermore, the implant surface exhibited low levels of carbon and trace elements and met ASTM standards (ASTM standards F136), this indicated ideal implant surface for tissue integration and better wetting property for clot formation on the surface of implants. The surface chemistry can also be customized by chemical treatment with HCl, NaOH and coating with hydroxyapatite, which makes the surface bioactive and ultimately improves the bone bonding properties in result encouraging bone growth (Heinl et al., 2008).

Surface wettability of the implant is a very important feature, because the hydrophilic implant surface offers an excellent biomaterial/host interface at the early healing stage and also during the process of osseointegration (Sartoretto et al., 2015). Study conducted by Zhao et al. suggests that the chemically pure and hydrophilic implant surface demonstrates superior osteoblastic differentiation factors such as alkaline phosphatase and osteocalcin (Zhao et al., 2005). Implant having good surface wettability also helps in adhesion of proteins and other macromolecules from blood and interstitial fluid at the first contact with the host and thereby results in better biological integration (Rupp et al., 2014; Sabetrasekh et al., 2010). In this study, titanium implant showed excellent surface wettability (Figs. 4 and 5), the dynamic contact angle test proved that the porous surface of the implant demonstrated excellent wettability from the time of initial contact of water droplet. The porous implant surface also provides a larger surface area for adhesion of proteins at the initial implant host interaction. The surface chemistry also indirectly affects the wettability of the surface, as surface impurities such as carbon and other trace elements significantly reduce hydrophilicity of the implant surface (Brunette et al., 2001). Hydrophilic surface exhibits higher oxide ions which react with OH ions of interstitial fluids and increase reactivity of the surface to interstitial macromolecules (Tengvall and Lundstrom, 1992; Gittens et al., 2014).

Although EBM produced restorations demonstrate a high degree of surface roughness (Fig. 2a and b), the struts are well formed, continuous, and very few internal pores were observed with μCT (Fig. 6). These micro pores mostly result from the feedstock powder rather than process settings (Murr et al., 2010). As mentioned above, the powder used in this study is produced by the gas atomization process. Sometimes there is a chance of inert gas getting entrapped within a powder particle. These pockets of gas get released when the powder particles are melted in EBM. Because of the very fast solidification rates, there may not have been sufficient time

for the entrapped gas to escape resulting in micro pores in the EBM part. The high surface roughness in EBM fabricated sample is because of the use of coarse alloy powder and high powder density (Murr et al., 2012). Even though the struts are well formed, the presence of numerous unmelted and partially fused alloy particles which creates hemispherical external porosity is the main concern as these defects may act as areas of stress concentration and can initiate crack (Elmagrabi et al., 2008). However, careful post processing procedures such as etching and coating will not only significantly reduce the stress points but also remove superficial unmelted powder particles which add to the strong initial implant stabilization because of the rough surface. Furthermore, certain dental restorations including fixed partial dentures and removable partial denture frameworks require smooth surface in order to have better patient comfort and to prevent food accumulation. Hence, removing this superficial layer by bead blasting and polishing may reduce stress concentration (Elmagrabi et al., 2008). Relatively smooth surface can also be achieved by changing the scaling of the CAD model and energy inputs (Harbe et al., 2013; Xiao et al., 2013) and orienting the build direction before the EBM process, due to the fact that the build surface demonstrates a comparatively smooth surface than the lateral surface and the resultant restoration can be finished and polished using bead blasting to a high degree of surface smoothness (Wu et al., 2010). On the other hand, internal porosities may severely affect the overall strength of the structure, but in this case the total internal porosity measured by μCT was very minimal (0.48113%) and internal structure appeared dense.

5. Conclusions

Rapid manufacturing technology has shown promising results for the fabrication of customized implants, it is not only time saving but also the structures are built accurately. The SEM analysis showed a rough lateral surface, which will be advantageous in case of dental implants, as it promotes bone ingrowth into small micro porosities and improved bone bonding. The surface chemical purity was proved to be acceptable because of negligible surface impurities and low levels of carbon. Results showed superior surface wetting property, which improves osteoblastic adhesion on to implant surface. EBM application for other intraoral dental restorations must be carefully addressed in order to reduce the surface roughness because the rough surface leads to food accumulation and further periodontal complications. However, the build surface showed comparatively smooth surface and further smoothness can be achieved by various finishing and polishing techniques such as 5-axis milling, computer controlled polishing and micro sand blasting. If developed further, this novel technology has the potential to become a technique of choice to be employed in the dental restoration fabrication.

Acknowledgments

The project was financially supported by Vice Deanship of Research Chairs, King Saud University, Riyadh, Kingdom of Saudi Arabia. Authors thank Mr. Mohamed A. Elsharawy for laboratory and technical assistance.

References

Al-Mesmar, H.S., Morgano, S.M., Mark, L.E., 1999. Investigation of the effect of three sprue designs on the porosity and the completeness of titanium cast removable partial denture frameworks. J. Prosthet. Dent. 82, 15–21.

Anusavice, K.J., 2003. Casting Investments and Procedures, Phillip's Science of Dental Materials, 11th ed. Saunders, St. Louis, Missouri, pp. 295–300.

Bibb, R., Eggbeer, D., Robert Williams, R., 2006. Rapid manufacture of removable partial denture frameworks. Rapid Prototyping J. 12, 95–99.

Biemond, J.E., Aquarius, R., Verdonschot, N., Buma, P., 2011. Frictional and bone ingrowth properties of engineered surface topographies produced by electron beam technology. Arch. Orthop. Trauma Surg. 131, 711–718.

Brunette, D.M., Tengvall, P., Textor, M., Thomsen, P., 2001. Titanium in medicine: material science, surface science, engineering, biological responses and medical applications. In: Textor, M., Sittig, C., Frauchiger, V., Tosatti, S., Brunette, D.M. (Eds.), Properties and Biological Significance of Natural Oxide Films on Titanium and its Alloys. Springer, New York, pp. 171–230.

Chahine, G., Koike, M., Okabe, T., Smith, P., Kovacevic, R., 2005. The design and production of Ti–6Al–4V ELI customized dental implant. J. Min. Metall. Mater. 60, 50–55.

De Peppo, G.M., Palmquist, A., Borchardt, P., Lenneras, M., Hyllner, J., Snis, A., Lausmaa, J., Thomsen, P., Karlsson, C., 2012. Free-form-fabricated commercially pure Ti and Ti6Al4V porous scaffolds support THE growth of human embryonic stem cell-derived mesodermal progenitors. Sci. World J., 1–14 Article ID 646417.

Einstein, P.A., Harvey, D.R., Simmons, P.J., 1963. The design of an experimental electron beam melting. J. Sci. Instrum. 40.

Elmagrabi, N., Che Hassan, C.H., Jaharah, A.G., Shuaeib, F.M., 2008. High speed milling of Ti–6Al–4V using coated carbide tools. Eur. J. Sci. Res. 22, 153–162.

Farooq, W.A., Tawfik, W., Al-Mutairi, F.N., Alahmed, Z.A., 2013. Qualitative analysis and plasma characteristics of soil from a desert area using LIBS technique. J. Opt. Soc. Korean 17, 548–558.

Gittens, R.A., Scheideler, L., Rupp, F., Hyzy, S.L., Geis-Gerstorfer, J., Schwartz, Z., Boyan, B.D., 2014. A review on the wettability of dental implant surfaces II: biological and clinical aspects. Acta Biomater. 10, 2907–2918.

Harbe, N.W., Heinl, P., Bordia, R.K., Korner, C., Fernandes, R.J., 2013. Maintenance of bone collagen phenotype by osteoblast-like cell in 3D periodic porous titanium (Ti–6Al–4V) structures fabricated by selective electron beam melting. Connect. Tissue Res. 10.

Haslauer, C.M., Springer, J.C., Harrysson, O.L., Loboa, E.G., Monteiro-Riviere, N.A., Marcellin-Little, D.J., 2010. In vitro biocompatibility of titanium alloy discs made using direct metal fabrication. Med. Eng. Phys. 32, 645–652.

Heinl, P., Rottmair, A., Korner, C., Singer, R.F., 2007. Cellular titanium by selective electron beam melting. Adv. Eng. Mater. 9, 360–364.

Heinl, P., Muller, L., Korner, C., Singer, R.F., Muller, F.A., 2008. Cellular Ti–6Al–4V structures with interconnected macro porosity for bone implants fabricated by selective electron beam melting. Acta Biomater. 4, 1536–1544.

Jamshidiniaa, M., Wangb, L., Tongb, W., Kovacevica, R., 2014. The bio-compatible dental implant designed by using non-stochastic-porosity produced by Electron Beam Melting (EBM). J. Mater. Process Technol. 214, 1728–1739.

Jamshidiniaa, M., Wangb, L., Tongb, W., Ajlounic, R., Kovacevica, R., 2015. Fatigue properties of a dental implant produced by electron beam melting (EBM). J. Mater. Process Technol. 226, 255–263.

Jevremovic, D., Kojic, V., Bogdanovic, G., Puskar, T., Eggbeer, D., Thomas, D., Williams, R., 2011. A selective laser melted Co–Cr alloy used for the rapid manufacture of removable partial denture frameworks- initial screening of biocompatibility. J. Serb. Chem. Soc. 76, 43–52.

Juechter, V., Scharowsky, T., Singer, R.F., Körner, C., 2014. Processing window and evaporation phenomena for Ti–6Al–4V produced by selective electron beam melting. Acta Mater. 76, 252–258.

Koike, M., Greer, P., Owen, K., Murr, L.E., Gaytan, S.M., Martinez, E., Okabe, T., 2011. Evaluation of titanium alloy fabricated using rapid prototyping technologies-electron beam melting and laser beam melting. Materials 4, 1776–1792.

Miguens, F.C., de Oliveira, M.L., Marins, R.V., de Lacerda, L.D., 2010. A new protocol to detect light elements in estuarine sediments by X-ray microanalysis (SEM/EDS). J. Electron Microsc. 59, 437–446.

Murr, L.E., Esquivel, E.V., Quinones, S.A., Gaytan, S.M., Lopez, M. I., Martinez, E.Y., Medina, F., Hernandez, D.H., Martinez, E., Martinez, J.L., Stafford, S.W., Brown, D.K., Hoppe, T., Meyers, W., Lindhe, U., Wicker, R.B., 2006. Microstructure and mechanical properties of electron beam rapid manufactured Ti–6Al–4V biomedical prototypes compared to wrought Ti–6Al–4V. Mater. Charact. 60, 96–105.

Murr, L.E., Quinones, S.A., Gaytan, S.M., Lopez, M.I., Rodela, A., Martinez, E.Y., Hernandez, D.H., Martinez, E., Medina, F., Wicker, R.B., 2009. Microstructure and mechanical behavior of Ti–6Al–4V produced by rapid-layer manufacturing, for biomedical applications. J. Mech. Behav. Biomed. Mater. 2, 20–32.

Murr, L.E., Gaytan, S.M., Ceylan, A., Martinez, E., Martinez, L.J., Hernandez, D.H., Machado, B.I., Ramirez, D.A., Medina, F., Collins, S., Wicker, R.B., 2010. Characterization of titanium aluminide alloy components fabricated by additive manufacturing using electron beam melting. Acta Mater. 58, 1887–1894.

Murr, L.E., Gaytan, S.M., Ramirez, D.A., Martinez, E., Hernandez, J., Amato, K.N., Shindo, P.W., Medina, F.R., Wicker, R.B., 2012. Metal fabrication by additive manufacturing using laser and electron beam melting technologies. J. Mater. Sci. Technol. 28, 1–14.

Parthasarathy, J., Starly, B., Raman, S., Christensen, A., 2010. Mechanical evaluation of porous titanium (Ti6Al4V) structures with electron beam melting (EBM). J. Mech. Behav. Biomed. Mater. 3, 249–259.

Ramakrishnaiah, R., Farooq, W.A., Al Kheraif, A.A., Qasim, S., Aldwayyan, A.S., 2012. Laser induced breakdown spectroscopic analysis of dental elastomeric impression materials. Middle East J. Sci. Res. 11, 1003–1008.

Rupp, F., Gittens, R.A., Scheideler, L., Marmur, A., Boyan, B.D., Schwartz, Z., Geis-Gerstorfer, J., 2014. A review on the wettability of dental implant surfaces I: theoretical and experimental aspects. Acta Biomater. 10, 2894–2906.

Sabetrasekh, R., Tiainen, H., Reseland, J.E., Will, J., Ellingsen, J.E., Lyngstadaas, S.P., Haugen, H.J., 2010. Impact of trace elements on biocompatibility of titanium scaffolds. Biomed. Mater. 5, 15003.

Sartoretto, S.C., Alves, A.T., Resende, R.F., Calasans-Maia, J., Granjeiro, J.M., Calasans-Maia, M.D., 2015. Early osseointegration driven by the surface chemistry and wettability of dental implants. J. Appl. Oral Sci. 23, 279–287.

Syam, W.P., Al-Shehri, H.A., Al-Ahmari, A.M., Al-Wazzan, K.A., 2012. Preliminary fabrication of thin-wall structure of Ti6Al4V for dental restoration by electron beam melting. Rapid Prototyping J. 18, 230–240.

Tengvall, P., Lundstrom, I., 1992. Physico-chemical considerations of titanium as a biomaterial. Clin. Mater. 9, 115–134.

Wu, J., Wang, X., Zhao, X., Zhang, C., Gao, Bo., 2010. A study on the fabrication method of removable partial denture framework by computer-aided design and rapid prototyping. Rapid Prototyping J. 18, 318–323.

Xiao, D., Yang, Y., Su, X., Wang, D., Sun, J., 2013. An integrated approach of topology optimized design and selective laser melting process for titanium implants materials. Bio-Med. Mater. Eng. 23, 433–445.

Yang, J., Cai, H., Lv, J., Zhang, K., Leng, H., Wang, Z., Liu, Z., 2014. Biomechanical and histological evaluation of roughened surface titanium screws fabricated by electron beam melting. PLoS One 9.

Zhao, G., Schwartz, Z., Wieland, M., Rupp, F., Geis-Gerstorfer, J., Cochran, D.L., Boyan, B.D., 2005. High surface energy enhances cell response to titanium substrate microstructure. J. Biomed. Mater. Res. A 74, 49–58.